Journal of Cluster Science (2020) 31:523–534
https://doi.org/10.1007/s10876-019-01669-7

ORIGINAL PAPER

Bioactive and Biocompatible Nature of Green Synthesized Zinc Oxide Nanoparticles from *Simarouba glauca* DC.: An Endemic Plant to Western Ghats, India

N. K. Hemanth Kumar[1] · M. Murali[2] · A. Satish[3] · S. Brijesh Singh[4] · H. G. Gowtham[4] · H. M. Mahesh[2] · T. R. Lakshmeesha[4] · K. N. Amruthesh[2] · Shobha Jagannath[1]

Received: 17 May 2019 / Published online: 17 September 2019

Abstract

Zinc-oxide nanoparticles (ZnO-NPs) synthesized from plant extracts are considered to possess superior biological activities compared to chemically synthesized nanoparticles and are of immediate interest to pharmaceutical and agriculture industries. The current study reports the green synthesis of ZnO-NPs from the aqueous leaf extract of *Simarouba glauca* for the first time. The physico-chemical characterization revealed hexagonal shaped nanoparticles with a size of $\sim$ 17 to 37 nm calculated by Scherrer's formula with a purity of 98.51%. The FT-IR results confirmed that functional groups present in the plant extract had coagulated well to form a metal oxide during the synthesis process. The antioxidant potential of green synthesized ZnO-NPs evaluated by different methods revealed significant ($p \leq 0.05$) radical scavenging activity (5% to 59%) with IC_{50} value falling between 400 and 500 μg mL^{-1} among the test methods. The green synthesized nanoparticles also inhibited the mitotic cell division up to 17.46% with increase in concentration. Further, the haemolytic assay by spectroscopic analysis affirmed the biocompatible nature of the nanoparticles which was also evidenced through SEM studies. The present findings indicate that the green synthesized ZnO-NPs from *S. glauca* possess antioxidant and antimitotic properties apart from possessing biocompatible nature to RBCs thereby warranting in vivo studies.

Electronic supplementary material The online version of this article (https://doi.org/10.1007/s10876-019-01669-7) contains supplementary material, which is available to authorized users.

✉ K. N. Amruthesh
dr.knamruthesh@botany.uni-mysore.ac.in

✉ Shobha Jagannath
shobhajags25@gmail.com

[1] Environmental Biology and Ecotoxicology Laboratory, Department of Studies in Botany, University of Mysore, Manasagangotri, Mysuru 570 006, Karnataka, India

[2] Applied Plant Pathology Laboratory, Department of Studies in Botany, University of Mysore, Manasagangotri, Mysuru 570 006, Karnataka, India

[3] Department of Studies in Food Science and Nutrition, University of Mysore, Manasagangotri, Mysuru 570 006, Karnataka, India

[4] Department of Studies in Biotechnology, University of Mysore, Manasagangotri, Mysuru 570 006, Karnataka, India

Graphic Abstract

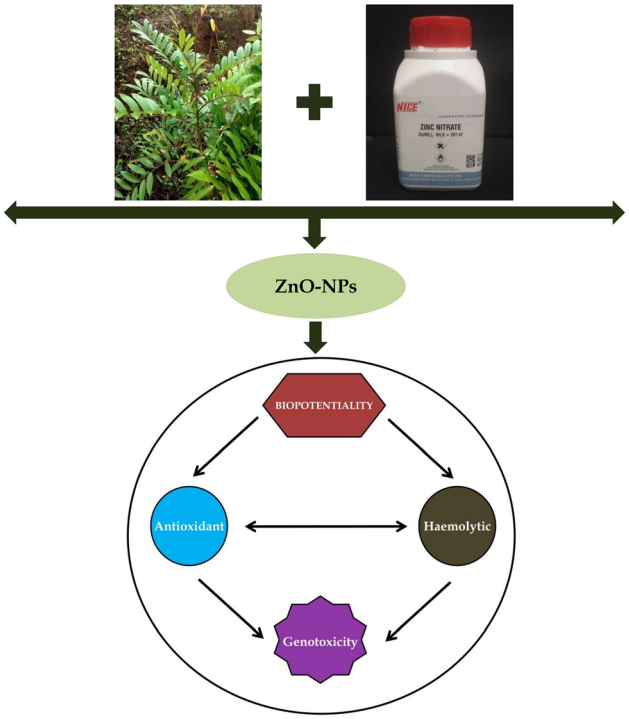

Keywords Antioxidant · Antimitotic · Chromosomal aberrations · Human RBCs · Nanoparticles

Introduction

Nanotechnology is a multidisciplinary field which includes all the branches of science and presently gaining importance in the field of pharmaceuticals. Nanotechnology mainly involves materials capable of manipulating properties of a substance at the molecular level [1]. At present, nanotechnology is rapidly expanding its area of research due to its broad range of applications in various disciplines primarily in medicines [2]. Nanoparticles are presently synthesized through physical, chemical, hybrid and biological methods [3, 4]. The physico-chemical techniques employed for the synthesis of nanoparticles have their drawbacks due to the use of toxic chemicals compared to the biosynthesis methods. Therefore the development of reliable, non-toxic and eco-friendly methods for the synthesis of nanoparticles is of utmost importance to expand their biological applications [4].

Among the metal oxide nanoparticles, zinc oxide nanoparticles (ZnO-NPs) are accepted globally due to their unique optical, electrical and biological properties [2, 5]. It has been noted that biosynthesized ZnO-NPs are more efficient in biological applications than chemically synthesized ZnO-NPs and is also listed in U.S. FDA (21CFR182.8991) as a safe drug [6, 7]. The undesirable effects of chemically synthesized nanoparticles have paved the way for plant-mediated biosynthesis of nanoparticles due to its stable and eco-friendly nature apart from their enhanced biological properties compared to chemically synthesized ones.

In recent years, aqueous plant extracts like *Aloe vera*, *Allium sativum*, *Rosmarinus officinalis*, *Ocimum basilicum*, *Jacaranda mimosifolia*, *Ceropegia candelebrum*, *Cardiospermum halicacabum*, *Cassia alata*, *Laurus nobilis*, etc., have been effectively used for the synthesis of ZnO-NPs which possess biological activities such as antimicrobial, antimitotic, antioxidant, anti-inflammatory and cytotoxic activities [2, 6–11]. The species of *Simarouba* are well known for its vast pharmacological properties as they possess many bioactive chemical constituents (glaucarubin, quassinoids, simaroubidin, simarolide, simarubin) which are mainly involved in hemostatic, anthelminthic, antiparasitic, antidysenteric, antipyretic and anti-cancerous properties [12, 13]. Among the *Simarouba* species, *S. glauca* is one of the pharmacologically important plant as it is used to cure fever, malaria, stomach and bowel disorders,

hemorrhages, amoebiasis, analgesic, antimicrobial, etc. [13]. Hence, due to its vast ethnopharmacological properties, the current study was carried out to green synthesize ZnO-NPs using aqueous leaf extract of *S. glauca* and to evaluate its bioactive potential.

Materials and Method

Collection of Plant Material

The healthy leaves of *Simarouba glauca* DC. was collected from the Western Ghats [Madikeri (12.41°N 75.73°E, elevation 1129 m)], Karnataka, India and identified with the help of Flora of Presidency of Madras [14].

Green Synthesis of Zinc Oxide Nanoparticles from *S. gluaca*

The collected leaf material of *S. glauca* was brought to the laboratory, washed thoroughly with sterile distilled water (SDW) and used for the synthesis of ZnO-NPs as reported in our previous studies [2]. In brief, 50 g of leaf material was extracted with 100 mL of SDW and filtered through Whatman No.1 filter paper. Approximately 50 mL of the filtrate was boiled to 60–80 °C on a magnetic stirrer and 5 gm of zinc nitrate hexahydrate was added and stirred until the mixture becomes a paste. The extract was collected in a ceramic crucible and combusted at 300 °C for 2 h in a furnace and the resulting powder (ZnO-NPs) was used throughout the study. Gas Chromatography-Mass Spectrometry (GC–MS) analysis of the aqueous extract was also carried out using Shimadzu GC–MS (Model QP2010S, Japan) to determine the phyto-constituents.

Characterization of Green Synthesized ZnO-NPs

The spectral analysis of green synthesized ZnO-NPs was carried out by measuring the optical density (OD) using Beckman Coulter, (DU739, Germany) scanning UV–Vis Spectrophotometer operated at a resolution of 1 nm between 200 and 800 nm. X-ray Powder Diffraction (XRD) patterns of the ZnO-NPs was performed on a Rigaku Desktop Miniflex II X-ray powder diffractometer with Cu kα radiation, (λ = 1.5406 A°) as the energy source. The diffracted intensities were recorded between 20 and 80° at 2θ angles. Maximum peak positions were compared with the standard files to identify the crystalline phase and the size of the particles was calculated using Scherrer's formula. Scanning electron microscopic (SEM) images of the ZnO-NPs was captured using HITACHI (S-3400 N, Japan) with 5 kV acceleration voltages. The energy dispersive spectroscopy (EDS) analysis was carried out on a HITACHI (Noran System 7, USA) system attached to SEM for the detection of metal ions present in ZnO-NPs. The Fourier Transform- Infrared (FT-IR) Spectroscopy was performed to note the changes in the binding properties in attenuated total reflection mode between the spectral range of 4000–400 cm^{-1} with a resolution of 4 cm^{-1}.

Antioxidant Potential of Green Synthesized ZnO-NPs from *S. gluaca*

Different radical scavenging methods were employed to study the antioxidant potential of green synthesized ZnO-NPs from *S. glauca* at various concentrations (100 to 500 μg mL^{-1}) (sonicated to avoid the agglomeration). The absorbance was measured spectrophotometrically against the related blank solutions. Each experiment was repeated thrice with appropriate control. The percentage of radical scavenging activity (RSA) was calculated using the following formula

$$\text{RSA } (\%) = \frac{\text{Absorbance of Control} - \text{Absorbance of Test sample}}{\text{Absorbance of Control}} \times 100$$

DPPH Radical Scavenging Activity

The DPPH free radical scavenging activity of green synthesized ZnO-NPs was carried out following the method of Serpen et al. [15]. About 3.5 mL of DPPH (0.1 mM) in methanol was taken containing different concentrations of ZnO-NPs and incubated at 37 ± 2 °C for 30 min under dark conditions. After incubation, the absorbance was read at 517 nm.

ABTS Radical Scavenging Assay

The ABTS free radical scavenging activity was carried out following the method of Shalaby and Shanab [16]. The ABTS solution was prepared by mixing 1:1 ratio of 2.45 mM potassium persulphate and 7 mM ABTS stock solution and kept overnight in the dark and diluted with methanol to maintain the absorbance at 734 nm after incubation. To 0.3 mL of different concentration of ZnO-NPs about 2.7 mL of ABTS solution was added and mixed thoroughly. The reaction mixture was incubated for 20 min under dark and the absorbance was read at 734 nm.

Hydrogen Peroxide Scavenging Assay

The ability of green synthesized ZnO-NPs to scavenge hydrogen peroxide was estimated following the method of Ruch et al. [17]. About 1 mL of different concentrations of ZnO-NPs was mixed thoroughly with 2 mL of hydrogen

peroxide solution (40 mM in phosphate buffer, pH 7.4). The reaction mixture was incubated for about 10 min and the absorbance was read at 230 nm.

Superoxide Radical Scavenging Assay

The superoxide radical scavenging assay was carried out following the method of Nishikimi et al. [18]. To 2 mL DMSO mixture (containing 5 mM NaOH on 0.1 mL water), 0.6 mL of different concentrations of ZnO-NPs was added along with 0.2 mL of nitroblue tetrazolium (NBT) (1 mg mL^{-1}). The reaction mixture was incubated for about 10 min and the absorbance was read at 560 nm.

Antimitotic Nature of Green Synthesized ZnO-NPs from *S. gluaca*

The genotoxicity of green synthesized ZnO-NPs was determined using onion (*Allium cepa* L.) assay following the method of Fiskesjo [19]. In brief, onion bulbs with fresh roots (4–5 day-old) were exposed to different concentrations of ZnO-NPs (100 to 500 µg mL^{-1}) and incubated for 24 h at 25 ± 2 °C. The root tips exposed to methotrexate and SDW served as positive and negative control, respectively. The incubated root tips (0.5–1.0 cm) were excised, washed with SDW and fixed in Carnoy's solution II (6:3:1 ratio of alcohol: chloroform: acetic acid) for 24 h. The fixed root tips were taken on a clean watch glass, stained with 2% aceto orcein and 1 N HCl and warmed under a spirit lamp and kept for 1 h. The stained root tips were squashed using 45% acetic acid on a clean glass slide and observed for cell division and chromosomal abnormalities under a microscope. The experiment was repeated thrice and 10 microscopic fields were observed for each replicate. The mitotic index of all the treatments was calculated using the formula:

$$\text{Mitotic Index } (\%) = \frac{\text{Number of Dividing Cells}}{\text{Total number of Cells}} \times 100$$

Fluorescence Microscopic Analysis

Control and treated *A. cepa* root tips were excised and treated with 1 N HCl for 2–3 min for hydrolysis of cell wall followed by repeated washings with SDW. The excised root tips were stained with nucleic acid specific

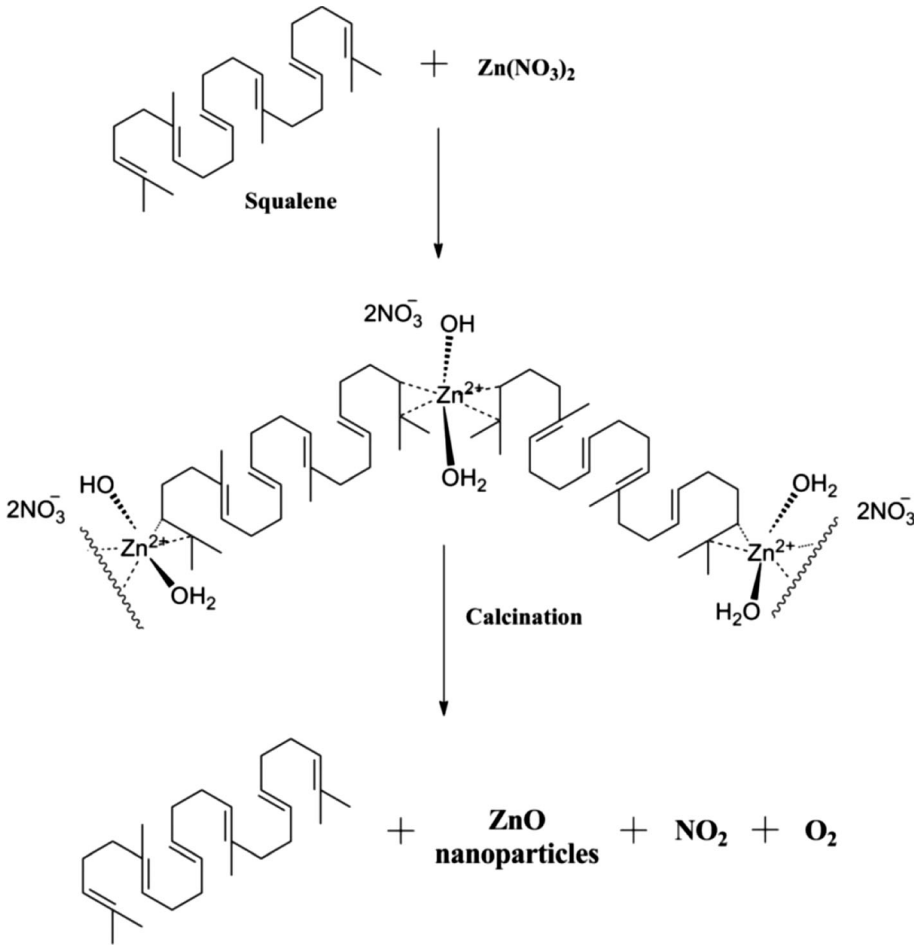

Fig. 1 Possible mechanism of formation of ZnO-NPs from *Simarouba glauca* aqueous leaf extract

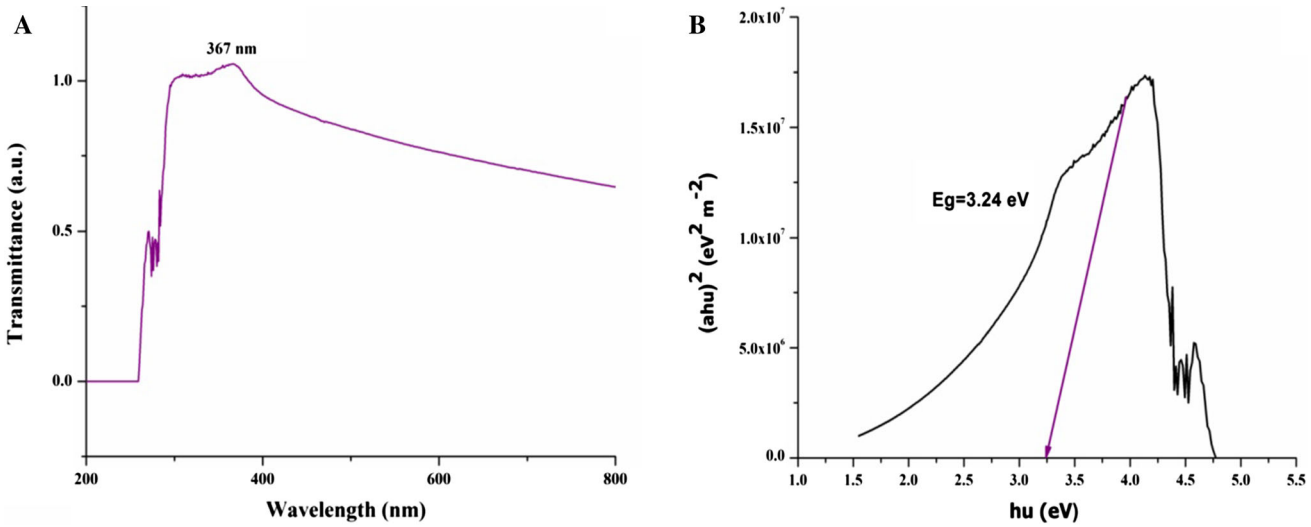

Fig. 2 The UV-absorption spectra (**a**) and energy band gap (**b**) of green synthesized ZnO-NPs from *Simarouba glauca*

stain acridine orange and propidium iodide (10 mg mL^{-1} in phosphate buffer) and incubated for 10 min under dark conditions. The stained root tips were squashed and observed for cell division and chromosomal abnormalities using Fluorescence microscope. The experiment was repeated thrice and 10 microscopic fields were observed for each replicate.

Biocompatible Nature of Green Synthesized ZnO-NPs from *S. gluaca*

The biocompatible nature of green synthesized ZnO-NPs was carried out by haemolytic assay on human red blood corpuscles (RBCs) according to the method of Surendra et al. [20] with some modifications. In brief, about 10 mL of blood sample (from healthy volunteers) was collected and centrifuged (1500 rpm for 5 min). The pellets (erythrocytes) were washed repeatedly with phosphate buffer saline (PBS) (pH 7.4) and resuspended again in PBS to give 5% hematocrit. For the haemolytic assay, various concentrations (100 to 500 µg mL^{-1} in PBS) of green synthesized ZnO-NPs was added to human erythrocyte diluted in PBS. The test samples were incubated at 37 °C for 1 h and centrifuged (1500 rpm for 5 min). The free hemoglobin content in the supernatant was measured spectrophotometrically at 540 nm. Each experiment was repeated thrice. Triton X-100 and PBS served as positive and negative control, respectively and the per cent haemolysis was calculated using the formula:

$$\text{Haemolysis } (\%) = \frac{\text{OD of Test sample} - \text{OD of PBS}}{\text{OD of PBS} - \text{OD of Triton X} - 100} \times 100$$

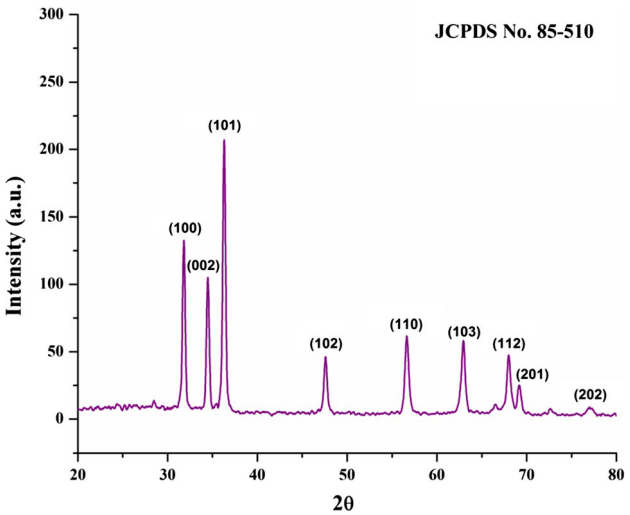

Fig. 3 X-ray Powder Diffraction analysis of green synthesized ZnO-NPs from *Simarouba glauca*

Effect of Green Synthesized ZnO-NPs from *S. gluaca* on RBCs Morphology

The change in morphology of RBCs upon ZnO-NPs treatment was carried out following the method of Kalita et al. [21] with some modifications. The RBCs treated with green-synthesized ZnO-NPs (for 1 h) along with respective controls were centrifuged at 1500 rpm for 5 min and the collected pellets were washed with PBS. The treated RBCs were then fixed with 5% formaldehyde solution for 3 h and subjected to dehydration using gradient ethanol series (25, 50, 75, 90 and 100%) with 10 min incubation for each selected concentrations. Triton X-100 and PBS served as

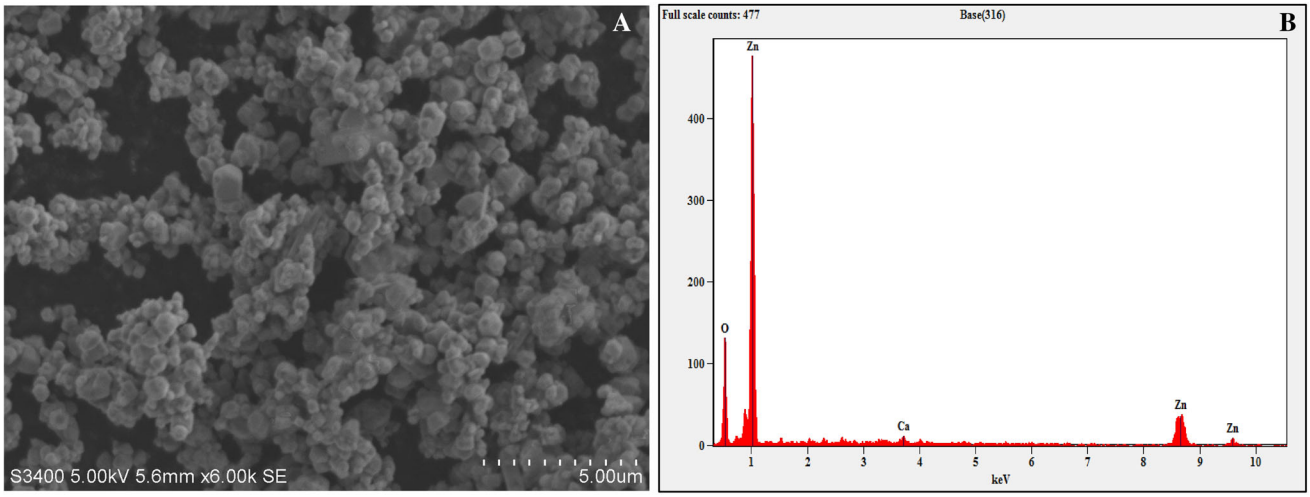

Fig. 4 Scanning electron microscopic (**a**) and energy dispersive spectroscopic (**b**) analysis of green synthesized ZnO-NPs from *Simarouba glauca*

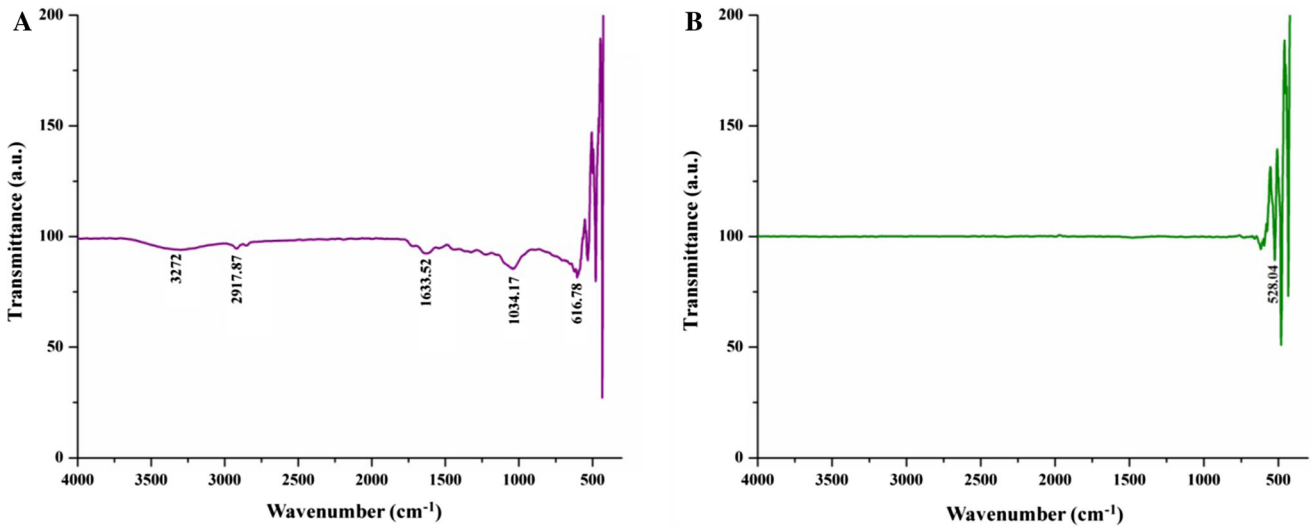

Fig. 5 FT-IR analysis of aqueous leaf extract of *Simarouba glauca* (**a**) and its green synthesized ZnO-NPs (**b**)

positive and negative control, respectively. After dehydration, the RBCs were evaporated to dryness in a desiccator. The obtained RBCs were observed for their morphology under SEM.

Statistical Analysis

The experimental data were statistically analyzed by subjecting to arcsine transformation and analysis of variance (ANOVA) using SPSS, version 17 (SPSS Inc., Chicago, IL). The significant differences between the treatments mean values were determined by Highest Significant Difference (HSD) obtained by Tukey's test at $p \leq 0.05$ levels.

Results and Discussion

Green Synthesis of Zinc Oxide Nanoparticles from *S. gluaca*

The GC–MS analysis of *S. glauca* aqueous leaf extract revealed the presence of six major peaks of different phytoconstituents (Suppl. Fig. 1). From the results, squalene a medicinally important bio-active compound was detected which belongs to triterpene (an aliphatic hydrocarbon) and is in accordance with previous reports [22, 23]. The detection of aliphatic group compound from GC–MS is in confirmation with peak observed under FT-IR studies of *S. gluaca* aqueous leaf extract obtained in the present study. To date there are no reports on the exact mechanism for the formation of ZnO-NPs from plant extracts but it has been

Table 1 Antioxidant potential of green synthesized ZnO-NPs from *Simarouba glauca*

Antioxidant Assays	ZnO-NPs (μg mL^{-1})					
	100	200	300	400	500	*IC_{50}
DPPH	5.58 ± 0.68^{c}	16.84 ± 0.42^{c}	28.97 ± 0.62^{d}	39.85 ± 1.04^{b}	52.46 ± 0.74^{c}	410.50
H_2O_2	11.37 ± 0.33^{a}	31.50 ± 0.60^{a}	43.58 ± 0.71^{a}	49.46 ± 0.63^{a}	60.77 ± 0.33^{a}	429.80
ABTS	9.03 ± 0.31^{b}	20.52 ± 0.35^{b}	32.50 ± 0.34^{c}	44.69 ± 0.65^{a}	59.56 ± 0.67^{ab}	430.10
Superoxide	8.62 ± 0.36^{b}	17.95 ± 0.58^{c}	36.01 ± 0.47^{b}	45.46 ± 0.86^{a}	57.39 ± 0.59^{b}	485.50

*The half maximal inhibitory concentration. Values are mean of three independent replicates (n = 3). ± indicate standard errors. Means followed by the same letter(s) within the same column are not significantly ($p \leq 0.05$) different according to Tukey's HSD

quoted that polar groups are responsible for the formation/synthesis of nanoparticles [24–26]. Hence, one of the possible adapted mechanisms for the capping effect of the plant extract during the formation of ZnO-NPs from aqueous leaf extract of *S. glauca* is dipicted in Fig. 1. During the formation of ZnO-NPs, zinc ions (Zn^{2+}) will cap with available phyto-constituents in plant extract to form a complex compound which undergoes direct decomposition at 300 °C in static air atmosphere finally leading in the formation of ZnO-NPs which is in corroboration with the studies of Karnan and Selvakumar [27] and Jafarirad et al. [28].

Characterization of Green Synthesized ZnO-NPs

The green synthesized ZnO-NPs from *S. glauca* were dispersed in SDW and were subjected to UV–Vis spectral analysis. The results of the spectral analysis revealed an absorption peak at 367 nm (Fig. 2a) with band gap energy of 3.24 eV (Fig. 2b). The results are in confirmation with the findings of Murali et al. [2] and Ni et al. [29], wherein green synthesized and chemically synthesized ZnO-NPs offered absorption peaks at 320 and 364 nm, respectively. It has been proved previously that, due to its absorption spectra (between 280 and 400 nm) and band gap energy (3.2 eV to 3.5 eV) ZnO-NPs are considered to be the main criteria for their beneficial aspects in biological and pharmaceutical fields [30, 31]. The X-ray Powder Diffraction analysis of green synthesized ZnO-NPs showed stiff and narrow diffraction peaks with no remarkable shift in the diffraction indicating that the crystalline product was without any impurities. The XRD patterns showed noticeable peaks at 31.73°, 34.45°, 36.26°, 47.59°, 56.56°, 62.94°, 67.92°, 69.12° and 76.86° correspond to (100), (002), (101), (102), (110), (103), (112), (201) and (202) planes of hexagonal wurtzite as shown in Fig. 3. The plane values of XRD patterns have good agreement with JCPDS No: 85-510 [32]. The size of the green synthesized ZnO-NPs of the present study calculated using Scherrer's formula was found between ~ 17 and 37 nm (Suppl. Table 1). The XRD results are in agreement with the findings of Murali et al. [2], wherein biosynthesized ZnO-NPs from *C. candelabrum* was of hexagonal wurtzite shape with 12–35 nm in size. The findings are also in accord with Lakshmeesha et al. [32], wherein ZnO-NPs synthesized from *Nerium oleander* offered stiff narrow diffraction peaks without any impurities. The images of green synthesized ZnO-NPs showed agglomeration of ZnO-NPs with hexagonal shape (Fig. 4a). The EDS analysis further confirmed that the green synthesized ZnO-NPs were of 98.51% purity (Suppl. Table 2) indicating that the process of green synthesis was carried out in accordance (Fig. 4b). The results of SEM and EDS for shape and purity are in accordance with the results obtained through XRD. Similarly, researchers have demonstrated that ZnO-NPs synthesized from plant extracts illustrate high purity of ZnO-NPs which have been confirmed through XRD, SEM and EDS analysis [2, 33, 34]. Further, FT-IR spectroscopy was carried out to study the change in the functional group

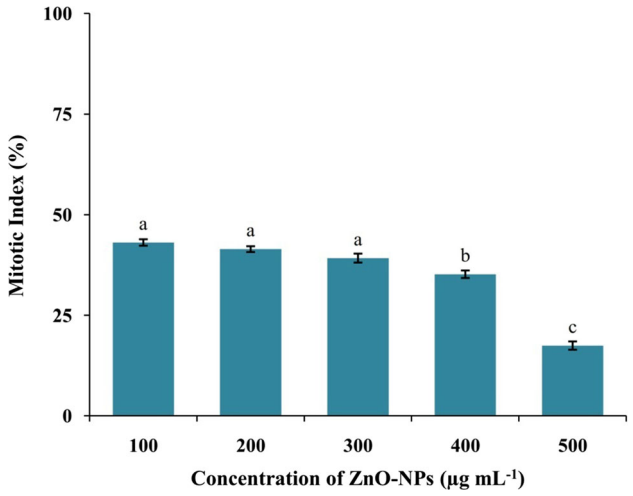

Fig. 6 Antimitotic potential of green synthesized ZnO-NPs from *Simarouba glauca*. Each value is the mean for three replicates (n = 3) and bars sharing the same letters are not significantly different ($p \leq 0.05$) according to Tukey's HSD (honest significant difference). The vertical bar indicates the standard error

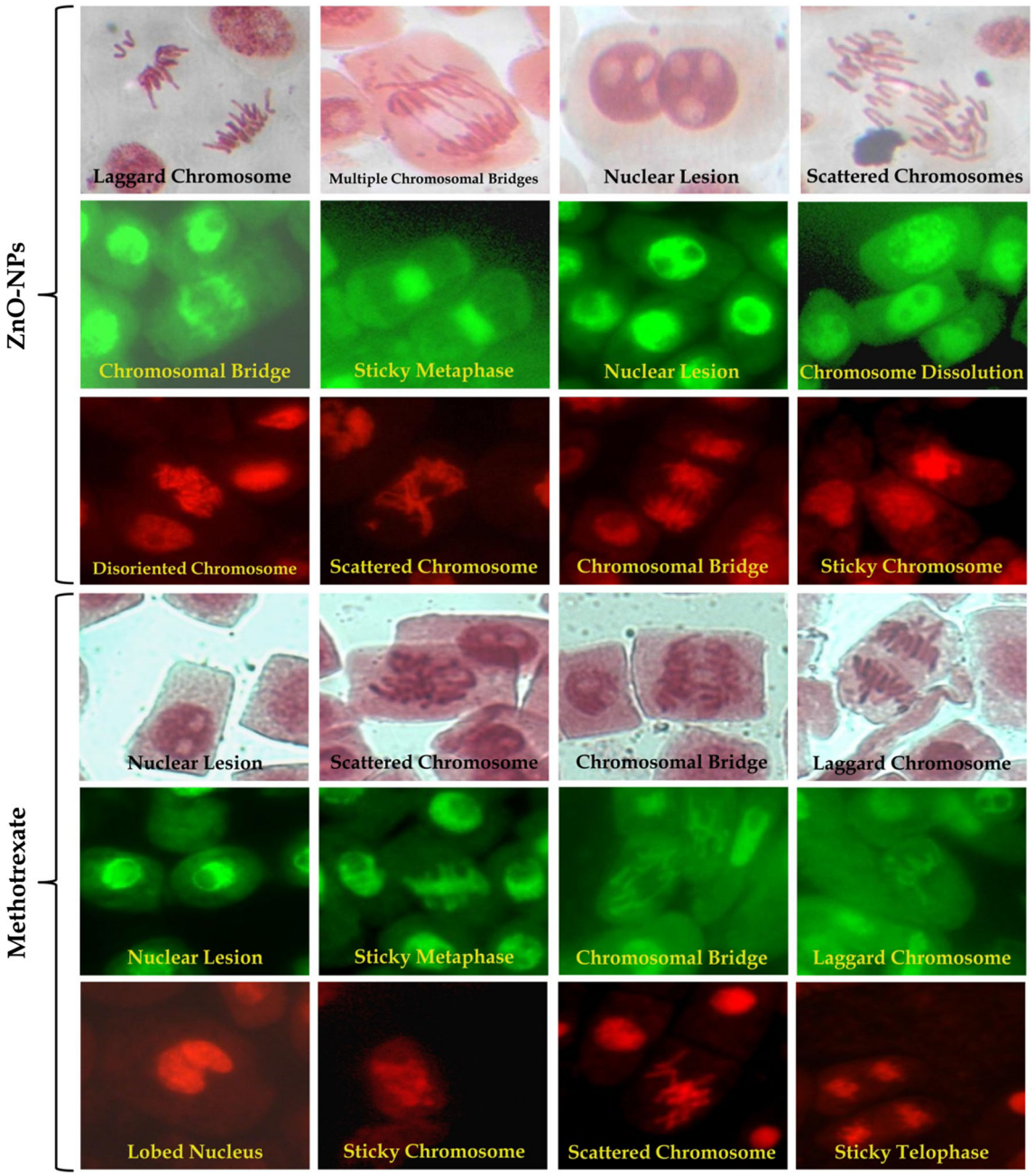

Fig. 7 Representative optical microscopic analysis revealing chromosomal abnormalities in *A. cepa* root meristem cells upon treatment with green synthesized ZnO-NPs and methotrexate. The microscopic images are representative of multiple experiments

during the bio-reduction of plant extract to ZnO-NPs (Fig. 5). The technique employed helps in identifying the functional groups present during the process of reduction and stabilization of plant extracts to ZnO-NPs [35]. The FT-IR spectrum of the ZnO-NPs showed a peak at 528.04 cm^{-1} which corresponds to metal oxide (M–O) bond and it is considered to be the characteristic peak of the metal nanoparticles. In plant extract, spectrum bands were observed at 3272 cm^{-1} [alcohol/phenol (OH/-H)], 2917.87 cm^{-1} [aliphatic (C–H)], 1633.52 cm^{-1} [primary amine (NH)], 1034.17 cm^{-1} [aliphatic amine (C–N)] and 616.78 cm^{-1} [alkyne (–C ≡ C–H)]. Further, the lack of the peaks around 3250 cm^{-1} in ZnO-NPs indicates that the green synthesized particles were free from moisture. It may be noted through FT-IR spectrum of ZnO-NPs that, functional groups present in plant extract had complexed well to form a metal oxide as indicated by the absence of major peaks between 600 and 400 cm^{-1}. Further, the results of FT-IR are in agreement with the findings of other researchers, wherein the absorption peak observed between

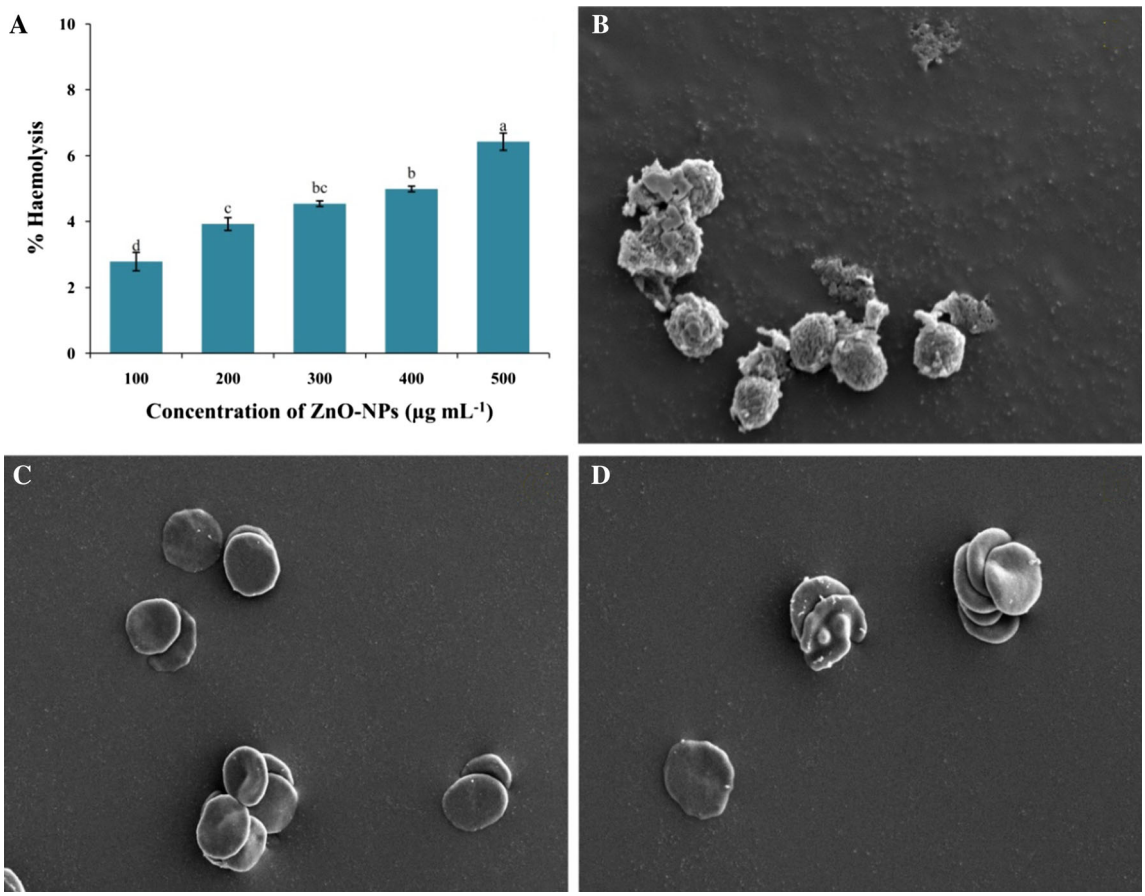

Fig. 8 Biocompatible nature of green synthesized ZnO-NPs *from Simarouba gluaca*. **a** Percentage of haemolysis measured by a spectrophotometer; SEM analysis of RBCs treated with **b** Triton X-100; **c** PBS; **d** Green synthesized ZnO-NPs. Each value is the mean for three replicates (n = 3) and bars sharing the same letters are not significantly different ($p \leq 0.05$) according to Tukey's HSD (honest significant difference). The vertical bar indicates the standard error

400 and 600 cm^{-1} is designated has a metal oxide bond [2, 26].

Antioxidant Potential of Green Synthesized ZnO-NPs from *S. gluaca*

Hydroxyl radicals are the most reactive form of free radicals responsible for DNA damage and lipid peroxidation which can pave the way to cancer and its related complications [36]. The results of antioxidant potential of green synthesized ZnO-NPS estimated by DPPH, ABTS, H_2O_2 and Superoxide radicals scavenging methods are given in Table 1. The RSA of green-synthesized ZnO-NPs from *S. gluaca* was found between 5 and 59% (among different methods) and the antioxidant potential increased with increase in the concentration of ZnO-NPs. The half maximal inhibitory concentration (IC_{50}) of RSA varied between 400 and 500 µg mL^{-1} among the test methods. The standard control (ascorbic acid) offered 75% inhibition at 50 µg mL^{-1}. The results are in agreement with other researchers, wherein plant extract mediated ZnO-NPs offered potent antioxidant activity [2, 7]. The results indicate that due to the encapsulation of secondary metabolites during the synthesis of ZnO-NPs has resulted in higher antioxidant potential of the nanoparticles and the same are in agreement with the findings of Suresh et al. [5].

Antimitotic Nature of Green Synthesized ZnO-NPs from *S. gluaca*

The antimitotic activity of green synthesized ZnO-NPs was studied using *Allium* assay. Onion is considered as a good bioindicator for genotoxicity and clastogenicity studies by environment protection agencies such as United Nations Environmental Programme (UNEP) and the United States Environmental Protection Agency (USEPA) [37]. The mitotic index decreased from 43.06 to 17.46% in the present study with an increase in the concentration of green synthesized ZnO-NPs from *S. glauca* compared to control (Fig. 6). The findings are in line with the results of Kumar et al. [38] and Sowbhagya and Ananda [39], wherein decrease in mitotic cell division was observed in onion root

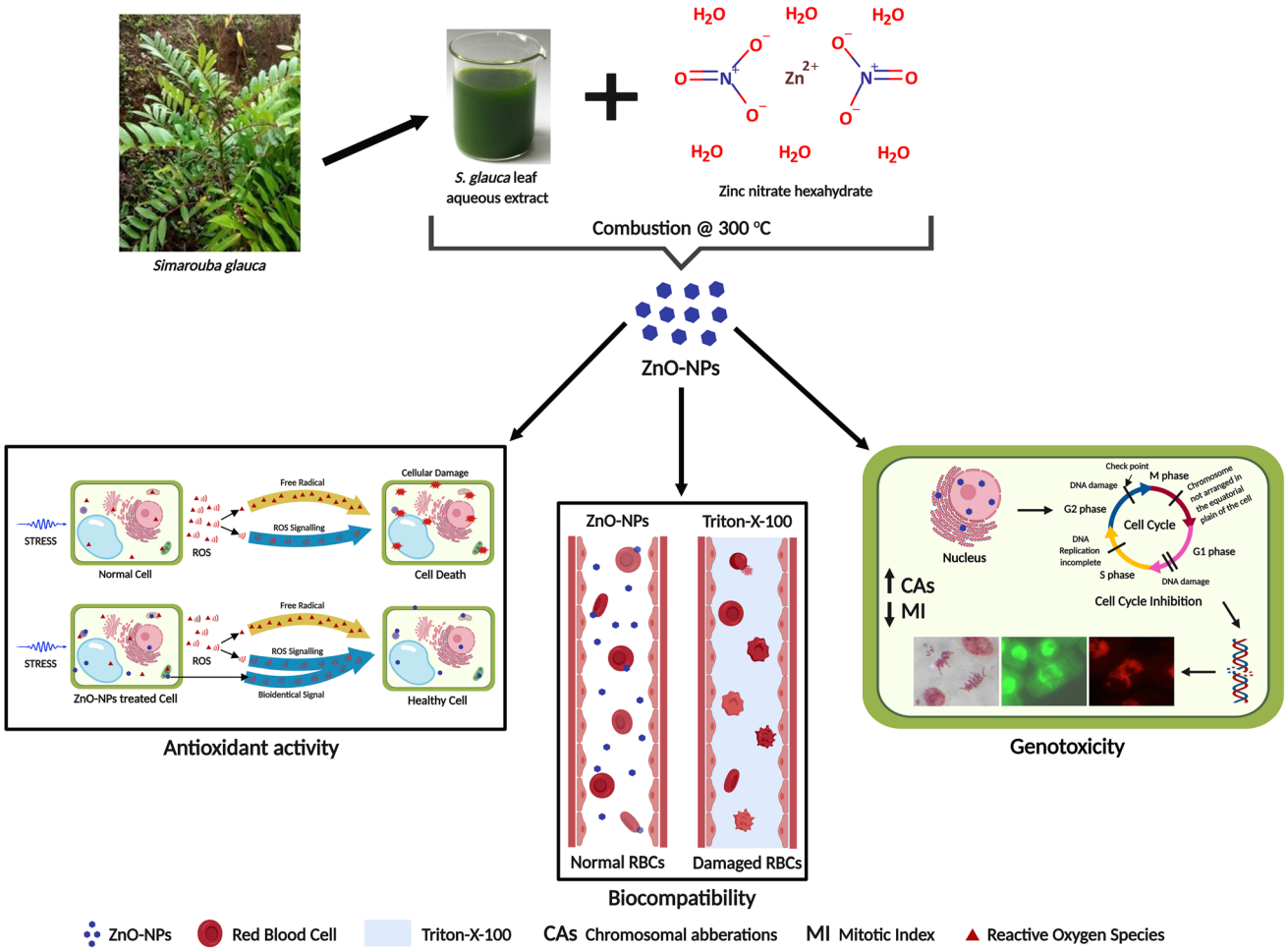

Fig. 9 Schematic representation of plausible mechanism of green synthesized ZnO-NPs from *S. glauca* interaction with cellular components resulting in induced oxidative stress, genotoxicity in *A. cepa* roots and biocompatibility towards RBCs

tips exposed to biologically and chemically synthesized ZnO-NPs, respectively. A mitotic index of 56% and 8% was observed in the negative and positive control, respectively. The decrease in the percentage of the mitotic index is asserted due to the genotoxic nature of green synthesized ZnO-NPs [40]. The chromosomal abnormalities were higher in ZnO-NPs and methotrexate treated root tips (Fig. 7), while normal cell divisions were observed upon SDW treatment (Suppl. Figure 1). Accordingly, the reduction in cell division is well correlated to the chromosomal abnormalities found upon treatment with ZnO-NPs [33, 39, 40].

Biocompatibility of Green Synthesized ZnO-NPs from *S. glauca*

Haemolysis is a sensitive and reliable study which provides the damaging or sensitizing effect of the drugs which are attached or encapsulated in RBCs before conducting the expensive and low-throughput animal studies [41]. Considering the potential antioxidant and cytotoxic nature of the ZnO-NPs, it becomes significantly relevant to determine the nature of ZnO-NPs on human RBCs. The green-synthesized nanoparticles offered haemolysis of 2.7 to 6.4% at 100 and 500 µg mL^{-1}, respectively (Fig. 8a). Concentration-dependent haemolysis was noted for ZnO-NPs indicating that the particles were nontoxic to human RBCs. It has been reported that 5% haemolysis is permissible for biomaterials [42] and accordingly up to 400 µg mL^{-1} of green-synthesized ZnO-NPs from *S. glauca* can be used for the haemolytic activity. Babu et al. [43] evaluated the size-dependent effect of ZnO-NPs at different concentrations and time interval and found that the ZnO-NPs which are below 50 nm in size offered better haemolysis compared to the ZnO-NPs which were above 100 nm in size. Likewise, it has been reported that chemically and biologically synthesized ZnO-NPs which offered antioxidant activity also possessed biocomapatible nature to RBCs [44, 45]. Dobrovolskaia et al. [46] have stated that nano-based drug carriers are rising as a substitute to present

drug delivery system and the results of the study confirm the biocompatible nature of these green synthesized ZnO-NPs from *S. gluaca* up to 400 μg mL^{-1}.

Effect of Green Synthesized ZnO-NPs from *S. gluaca* on RBCs Morphology

The biconcave shape of RBCs tends to be similar or altered when they interact upon non-toxic and toxic substances, respectively. The surface topography of RBCs captured through SEM showed changes in their morphology when they were exposed to Triton X- 100 (Fig. 8b), while the surface morphology remained unaltered when exposed to PBS (Fig. 8c) and green-synthesized ZnO-NPs (Fig. 8d) there by coinciding with the results of haemolysis. Similarly, size dependent biocomaptible nature of ZnO-NPs have been reported on RBCs by Babu et al. [43].

Conclusion

This is the first report on the green synthesis of ZnO-NPs from any of the *Simarouba* species that too from *S. glauca*. The green synthesized ZnO-NPs when subjected to physico-chemical characterization revealed that the nanoparticles were of 98.51% purity with ~ 17 to 37 nm in size. The green synthesized ZnO-NPs offered significant antioxidant and antimitotic properties including biocompatible nature to human RBCs. Figure 9 represents the overall plausible mechanism involved in the bioactive potential of green synthesized ZnO-NPs from *S. glauca* upon interaction with the cells. The results confirm bioactive as well as biocompatible nature of green synthesized ZnO-NPs from *S. glauca* thereby warranting in vivo and preclinical studies.

Acknowledgements The author M. Murali would like to acknowledge the University Grants Commission (UGC)- New Delhi, India for providing the financial support under UGC Post-Doctoral Fellowship (No. F/PDFSS-2015-17-KAR-11846). The authors are also thankful to University with Potential for Excellence (UPE) Project authorities and Department of Studies in Botany, University of Mysore for providing facilities.

References

1. M. Fakruddin, Z. Hossain, and H. Afroz (2012). *J. Nanobiotechnol.* **10**, 31.
2. M. Murali, C. Mahendra, Nagabhushan, N. Rajashekar, M. S. Sudarshana, K. A. Raveesha and K. N. Amruthesh (2017). *Spectrochim Acta A Mol. Biomol. Spectrosc.* **15**, 104.
3. P. Mohanpuria, N. K. Rana, and S. K. Yadav (2008). *J. Nanoparticles Res.* **10**, 507.
4. X. Li, H. Xu, Z. Chen, and G. Chen (2011). *J. Nanomaterials*, **2011**, 270974.
5. D. Suresh, R. M. Shobharani, P. C. Nethravathi, M. A. Pavan-Kumar, H. Nagabhushana, and S. C. Sharma (2015). *Spectrochim Acta A Mol. Biomol. Spectrosc.* **141**, 128.
6. S. Gunalan, R. Sivaraj, and V. Rajendran (2012). *Prog Nat Sci Mater Int.* **22**, 693.
7. M. Stan, A. Popa, D. Toloman, T. D. Silipas, and D. C. Vodnar (2016). *Acta. Metal. Sin.* **29**, 228.
8. D. Sharma, M. I. Sabela, S. Kanchi, P. S. Mdluli, G. Singh, T. A. Stenstrom, and K. Bisetty (2016). *J. Photochem. Photobiol. B: Biol. B.* **162**, 199.
9. K. Nithya and S. Kalyanasundharam (2019). *OpenNano.* **1**, 100024.
10. A. Happy, M. Soumya, S. V. Kumar, S. Rajeshkumar, R. D. Sheba, T. Lakshmi, and V. D. Nallaswamy (2019). *Biochem. Biophy. Rep.* **1**, 208.
11. S. Fakhari, M. Jamzad, and H. Kabiri Fard (2019). *Green Chem. Lett. Rev.* **2**, 19.
12. P. S. Mansi and D. K. Gaikwad (2011). *J. Pharm. Sci. Res.* **3**, 1195.
13. K. Ashwani, T. Gaurav, S. Sunayana, V. Kumar, and R. Pundir (2014). *Int. J. Pharmacognosy* **1**, 735.
14. J. S. Gamble *Flora of the Presidency of Madras*, vol. 3 (BSI, Calcutta, 1935).
15. A. Serpen, E. Capuano, V. Fogliano, and V. Gokmen (2007). *J. Agri. Food Chem.* **55**, 7676.
16. E. A. Shalaby and S. M. M. Shanab (2013). *Indian J. Geo-Mar Sci.* **42**, 556.
17. R. J. Ruch, S. J. Cheng, and E. Klaunig (1989). *Carcinogenesis* **10**, 1003.
18. M. Nishikimi, N. A. Rao, and K. Yagi (1972). *Biochem. Biophys. Res. Commun.* **46**, 849.
19. G. Fiskesjo (1985). *Hereditas* **102**, 99.
20. T. V. Surendra, S. M. Roopan, N. A. Al-Dhabi, M. V. Arasu, G. Sarkar, and K. Suthindhiran (2016). *Nanoscale Res. Lett.* **11**, 546.
21. S. Kalita, R. Kandimalla, B. Devi, B. Kalita, K. Kalita, M. Deka, A. C. Kataki, A. Sharma, and J. Kotoky (2017). *RSC Adv.* **7**, 1749.
22. S. Passi, O. De Pita, P. Puddu, and G. P. Littarru (2002). *Free Radic. Res.* **36**, 477.
23. B. Auffray (2007). *Int. J. Cosmet. Sci.* **29**, 29.
24. L. Medina-Ramirez, S. Bashir, Z. Luo, and J. L. Liu (2009). *Colloids Surf. B.* **73**, 185.
25. A. K. Jha and K. Prasad (2010). *Int. J. Green Nanotechnol. Phys. Chem.* **1**, 110.
26. R. Yuvakkumar, J. Suresh, A. J. Nathanael, M. Sundrarajan, and S. I. Hong (2014). *Mater. Lett.* **1**, 170.
27. T. Karnanm and S. A. Selvakumar (2016). *J. Mol. Struct.* **5**, 358.
28. S. Jafarirad, M. Mehrabi, B. Divband, and M. Kosari-Nasab (2016). *Mater. Sci. Eng. C.* **59**, 296.
29. Y. H. Ni, X. W. Wei, J. M. Hong, and Y. Ye (2005). *Mater. Sci. Eng. B.* **151**, 42.
30. R. Seshadri, in: Rao A CNR, Muller AK Cheetham (eds.), *The Chemistry of Nanomaterials*, vol 1, (Wiley-VCH Verlag GmbH, Weinheim 2004), p. 94.
31. A. Sirelkhatim, S. Mahmud, A. Seeni, N. H. M. Kaus, L. C. Ann, S. K. M. Bakhori, H. Hasan, and D. Mohamed (2015). *Nano-Micro Lett.* **7**, 219.
32. T. R. Lakshmeesha, M. K. Sateesh, B. D. Prasad, S. C. Sharma, D. Kavyashree, M. Chandrashekar, and H. Nagabushana (2014). *Cryst. Growth Des.* **14**, 4068.
33. C. Mahendra, M. Murali, G. Manasa, P. Ponnamma, M. R. Abhilash, T. R. Lakshmeesha, A. Satish, K. N. Amruthesh, and M. S. Sudarshana (2017). *Microbial Pathogenesis.* **110**, 620.
34. H. Sawada, R. Wang, and A. W. Sleight (1996). *J. Solid. State Chem.* **122**, 150.

35. S. R. Senthilkumar and T. Sivakumar (2015). *Int. J. Pharm. Sci.* **6**, 461.
36. V. Lobo, A. Patil, A. Phatak, and N. Chandra (2010). *Pharmacognosy Rev.* **4**, 118.
37. A. Thenmozhi, A. Nagalakshmi, and U. Mahadeva Rao (2011). *Int. J. Sci. Technol* **1**, 26–47.
38. N. H. Kumar, J. D. Andia, S. Manjunatha, M. Murali, K. N. Amruthesh, and S. Jagannath (2018). *Biocatal. Agricult. Biotechnol.* **1**, 101024.
39. S. Ananda Soubhagya (2014). *Am. Chem. Sci. J.* **4**, 616.
40. T. C. Taranath, B. N. Patil, T. U. Santosh, and B. S. Sharath (2015). *Env. Sci. Pol. Res.* **22**, 8611.
41. D. Pan, O. Vargas-Morales, B. Zern, A. C. Anselmo, V. Gupta, M. Zakrewsky, S. Mitragotri, and V. Muzykantov (2016). *PloS ONE* **11**, 0152074.
42. J. Autian in R. Kronenthal (ed.), *Polymers in Medicine and Surgery*, vol. 8 (Springer, New York, 1975), pp. 181–203.
43. E. P. Babu, A. Subastri, A. Suyavaran, K. Premkumar, V. Sujatha, B. Aristatile, G. M. Alshammari, V. Dharuman, and C. Thirunavukkarasu (2017). *Sci. Rep.* **7**, 4203.
44. D. Das, B. C. Nath, P. Phukon, and S. K. Dolui (2013). *Colloids Surf. B.* **111**, 556–560.
45. G. K. Prashanth, P. A. Prashanth, B. M. Nagabhushana, S. Ananda, H. G. Nagendra, and C. Rajendra Singh (2016). *Adv. Sci. Eng. Med.* **8**, 306–313.
46. M. A. Dobrovolskaia, J. D. Clogston, B. W. Neun, J. B. Hall, A. K. Patri, and S. E. McNeil (2008). *Nano Lett.* **8**, 2180.